International Journal of Nanomedicine

Dovepress
open access to scientific and medical research

Open Access Full Text Article

ORIGINAL RESEARCH

Selenium Biofortification Enhanced miR167a Expression in Broccoli Extracellular Vesicles Inducing Apoptosis in Human Pancreatic Cancer Cells by Targeting IRS1

Xiaohui Wang[1,*], Bo Wu[2,*], Guogen Sun[3], Wenxi He[4], Jia Gao[1], Teng Huang[1], Jing Liu[1], Qing Zhou[1], Xiaoyu He[5], Shu Zhang[1], Zixiong Zhang[2], He Zhu[1]

[1]The Center for Biomedical Research, Department of Respiratory and Critical Care Medicine, NHC Key Laboratory of Respiratory Diseases, Tongji Hospital, Tongji Medical College, Huazhong University of Sciences and Technology, Wuhan, Hubei, People's Republic of China; [2]The Central Hospital of Enshi Tujia and Miao Autonomous Prefecture, Hubei Selenium and Human Health Institute, Enshi, Hubei, People's Republic of China; [3]Hubei Selenium and Human Health Institute, Enshi, Hubei, People's Republic of China; [4]Department of Pharmacy, Tongji Hospital, Tongji Medical College, Huazhong University of Science and Technology, Wuhan, Hubei Province, People's Republic of China; [5]Branch of National Clinical Research Center for Metabolic Diseases, Department of Endocrinology, Tongji Hospital, Tongji Medical College, Huazhong University of Science and Technology, Wuhan, Hubei, People's Republic of China

*These authors contributed equally to this work

Correspondence: Zixiong Zhang, The Central Hospital of Enshi Tujia and Miao Autonomous Prefecture, Hubei Selenium and Human Health Institute, No. 158, Muyang Avenue, Enshi, Hubei, People's Republic of China, Email 596099670@qq.com; He Zhu, The Center for Biomedical Research, Department of Respiratory and Critical Care Medicine, NHC Key Laboratory of Respiratory Diseases, Tongji Hospital, Tongji Medical College, Huazhong University of Sciences and Technology, No. 1095 Jiefang Avenue, Wuhan, Hubei, People's Republic of China, Email Zhuh@tjh.tjmu.edu.cn

Purpose: Pancreatic adenocarcinoma (PAAD) presents an extremely high morbidity and mortality rate. Broccoli has excellent anti-cancer properties. However, the dosage and serious side effects still limit the application of broccoli and its derivatives for cancer therapy. Recently, extracellular vesicles (EVs) derived from plants are emerging as novel therapeutic agents. Thus, we conducted this study to determine the effectiveness of EVs isolated from Se-riched broccoli (Se-BDEVs) and conventional broccoli (cBDEVs) for the treatment of PAAD.

Methods: In this study, we first isolated Se-BDEVs and cBDEVs by a differential centrifugation method, and characterized them by using nanoparticle tracking analysis (NTA) and transmission electron microscopy (TEM). Then, miRNA-seq was combined with target genes prediction, and functional enrichment analysis to reveal the potential function of Se-BDEVs and cBDEVs. Finally, the functional verification was conducted in PANC-1 cells.

Results: Se-BDEVs and cBDEVs exhibited similar characteristics in size and morphology. Subsequent miRNA-seq revealed the expression of miRNAs in Se-BDEVs and cBDEVs. Using a combination of miRNA target prediction and KEGG functional analysis, we found miRNAs in Se-BDEVs and cBDEVs may play an important role in treating pancreatic cancer. Indeed, our in vitro study showed that Se-BDEVs had greater anti-PAAD potency than cBDEVs due to increased bna-miR167a_R-2 (miR167a) expression. Transfection with miR167a mimics significantly induced apoptosis of PANC-1 cells. Mechanistically, further bioinformatics analysis showed that *IRS1*, which is involved in the PI3K-AKT pathway, is the key target gene of miR167a.

Conclusion: This study highlights the role of miR167a transported by Se-BDEVs which could be a new tool for counteracting tumorigenesis.

Keywords: selenium, broccoli, extracellular vesicles, apoptosis, pancreatic cancer

Introduction

Pancreatic cancer is one of the deadliest and least therapeutically approachable malignancies with a 5-year survival rate of 5–10%.[1,2] Currently, a few drugs have been developed to treat pancreatic cancer; however, they have not been satisfactorily conclusive,[3] because the potential drug resistance allows pancreatic cancer to evade cell death under various

Received: 9 November 2022
Accepted: 19 April 2023
Published: 9 May 2023

Graphical Abstract

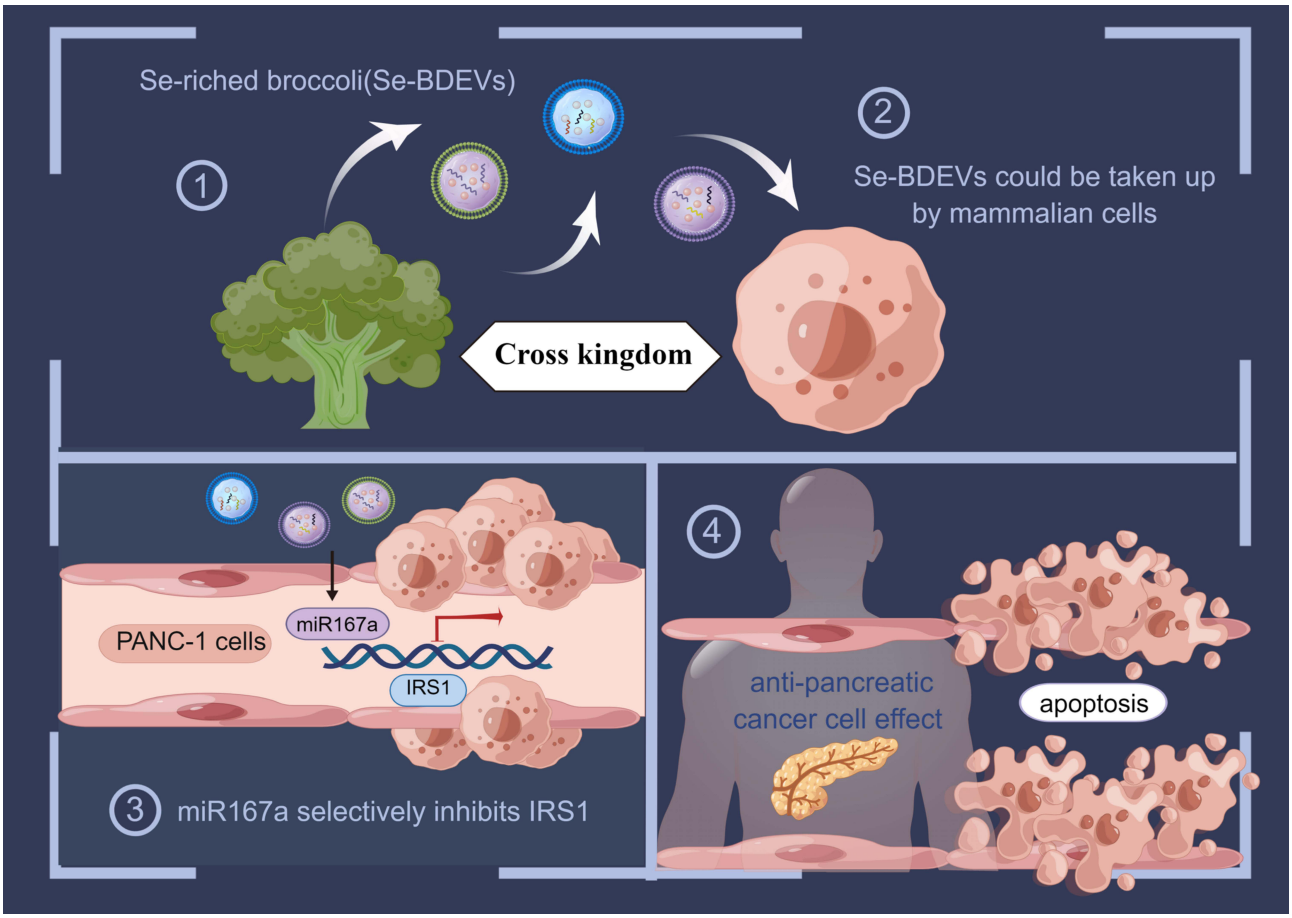

survival mechanisms.[1] Therefore, new therapeutic strategies are still urgently needed to improve the therapeutic effect of pancreatic cancer.

Recently, extracellular vesicles (EVs) secreted by living cells have a variety of well-studied functions in intercellular communication,[4,5] signal transduction,[6] and tumor development,[4,7] due to the ability to transport various types of bioactive substances, including nucleic acids,[6,8] proteins,[9] and lipids.[10,11] In addition, engineering modifications have enabled EVs to acquire powerful plasticities, such as better targeting, enhanced biocompatibility, and lower toxicity.[12] Furthermore, an increasing number of studies have reported the existence of plant-derived EVs with properties similar to mammalians.[13–16] For example, asparagus cochinchinensis-derived EVs can inhibit the proliferation of hepatocellular carcinoma cells with a better safety profile.[17] Broccoli-derived EVs (BDEVs) as nanocarriers for the delivery of sulforaphane demonstrate a novel approach to the treatment of skin cancer.[18] Notably, these green medicine therapy strategies are used as a new therapeutic approach because of their biocompatible, cost-effective, eco-friendly, and mass-produced platforms.[19–21]

Broccoli, a prominent member of the *Brassica genus* family, is popular on dinner tables and is widely thought to have anti-cancer properties.[22] Several epidemiologic studies have highlighted the anticarcinogenic effect of broccoli and its by-products (such as sulforaphane and isothiocyanates).[23] Recent clinical trial research with 40 pancreatic adenocarcinoma (PAAD) patients also revealed that broccoli sulforaphane significantly reduced PAAD-related mortality. However, dosage and serious side effects limit the application of those broccoli derivatives.[24]

Additionally, selenium (Se) is an essential trace element that functions through selenoproteins whether in plants or animals.[25] Se biofortification has been proven that not only increases the phenolic compound content and flavonoids in broccoli but also accumulate two active anticancer agents (sulforaphane and Se-methylselenocysteine).[26,27] Nonetheless, no research has been conducted to date to establish the effect of Se on BDEVs.

In this study, BDEVs isolated from Se-riched broccoli (Se-BDEVs) or conventional broccoli (cBDEVs) were identified and characterized, and their miRNAs were profiled for expression using miRNA sequencing (miRNA-seq). The bioinformatic results, combined with target genes (TGs) prediction and functional analysis, revealed that BDEVs may play a crucial role in "pancreatic cancer". Indeed, Se-BDEVs showed stronger anti-PAAD potency than cBDEVs because of the highly expressed miR167a. Our in vitro study further demonstrated that miR167a induced PAAD apoptosis by targeting IRS1. Collectedly, our study provides novel insights into cross-kingdom regulation and highlights the role of microRNAs transported by Se-BELNs as natural bioactive plant compounds which would be a safer and economical alternative for counteracting tumorigenesis.

Materials and Methods

Broccoli Harvest and Sampling

Se-enriched broccoli and conventional broccoli were provided by Hubei Selenium and Human Health Institute, Enshi, Hubei, China. Se content in Se-enriched broccoli is 25.6 mg/kg, whereas Se element content in conventional broccoli is less than 0.1 mg/kg.

Isolation and Purification of BDEVs

Se-BDEVs and cBDEVs were isolated using the differential centrifugation method (Figure 1), as described previously.[28] Briefly, carefully washed fresh broccoli was cut into many small pieces and put into a juice blender (Hurom, South Korea). Subsequently, the juice was strained with a colander and collected. The collected fluid was centrifuged serially at 1200 g for 20 min, 3000 g for 20 min, and 10,000 g for 60 min to remove pellet cells and debris. Then, the obtained supernatant was ultracentrifuged at 150,000 g for 90 min at 4 °C to collect precipitates which are plant-derived EVs. The BDEVs pellet was washed with phosphate-buffered saline (PBS) and ultracentrifuged at 150,000 g for another 1 h. All

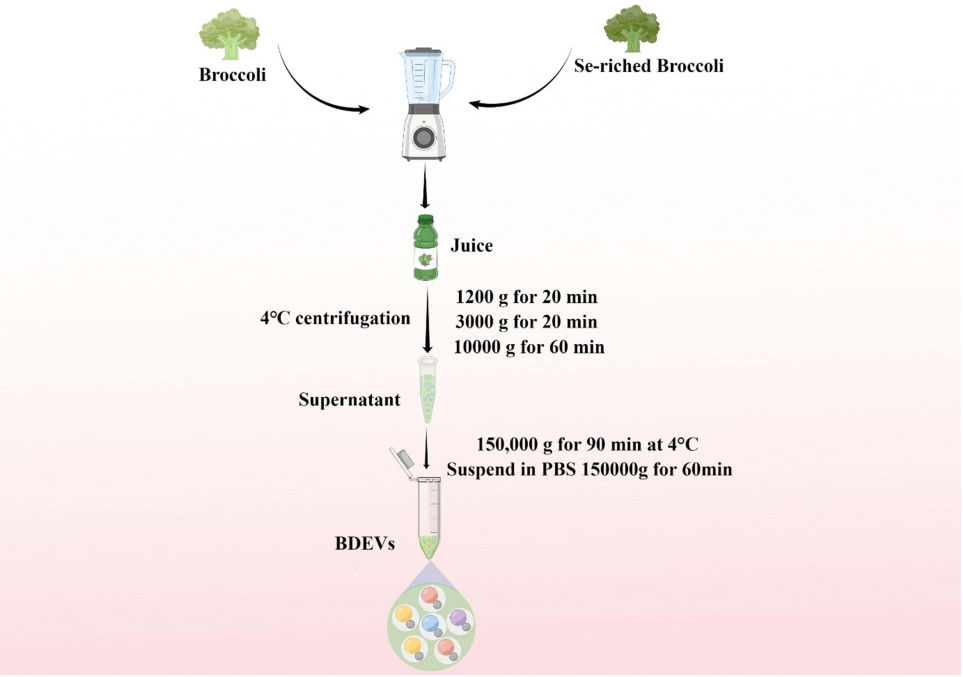

Figure 1 Schematic illustration of the isolation of extracellular vesicles derived from Se-riched broccoli (Se-BDEVs) and conventional broccoli (cBDEVs).

centrifugation temperatures were set to 4 °C. Finally, the obtained Se-BDEVs and cBDEVs were resuspended in sterile PBS stored at −80 °C until use. The quantity of Se-BDEVs and cBDEVs protein content was determined by the bicinchoninic acid (BCA) assay (Beyotime, China) method as the previous study did.[29]

BDEVs Characterization

As previously reported,[30] nanoparticle tracking analysis (NTA) and transmission electron microscopy (TEM) were used to characterize BDEVs. The size, distribution, and concentration of Se-BDEVs and cBDEVs were measured by NTA analysis (ZetaView, Particle Metrix, Germany). Briefly, EVs re-suspended in 50 μL PBS were further diluted to 300-fold to achieve between 20 and 100 objects per frame and detected by NanoSight NS-300 (Malvern Panalytical, Malvern, UK).

For TEM imaging, Se-BDEVs and cBDEVs were fixed with glutaraldehyde (Sigma Aldrich, USA) and stained with phosphotungstic acid (Sigma Aldrich, USA) on carbon-coated grids. The prepared samples were observed under an electron microscope HT7700 TEM (Hitachi, Japan) at 80 kV.

BDEVs Labeling and Cellular Uptake

Purified BDEVs were labeled with the PKH26 using the Fluorescent Cell Linker kit (Sigma-Aldrich, St. Louis, MO, USA). The same amount of BDEVs were mixed with the dye and incubated at 37 °C for 30 min. Then, PKH26-labeled BDEVs were collected by centrifugation at 150,000 g for 1 h and resuspended in PBS for further experiments. Then, the 293T cells were incubated with PKH26-labeled EVs at graded concentrations (10, 20, and 40 ng/μL quantitative by protein) for 24 h. The fluorescence was observed by fluorescence microscopy (Leica, Germany). In addition, the PANC-1 cells were treated with PKH67-labeled BDEVs (40 ng/μL) for 30 min, 1, 2, 4, and 6 h. The fluorescence was observed by Confocal microscopy (Nikon, Japan).

Cell Culture and Transfection

Human embryonic kidney 293 T cells (ATCC, CRL-3216) were grown in DMEM media containing 10% FBS and 1% penicillin/streptomycin. Human pancreatic cancer cells PANC-1 (ATCC, CRL-1469) were grown in 1640 media supplemented with 10% FBS and 1% penicillin/streptomycin. All cell culture reagents were obtained from Gibco (ThermoFisher, USA). All cell lines were incubated at 37 °C with 5% CO_2.

Transfections for PANC-1 cells were carried out using Lipofectamine 3000 (ThermoFisher, USA) as in our previous study.[31] MiR167a mimics were constructed according to the miRNA-seq data: 5'-TGAAGCTGCCAGCATGATCT-3'.

Cell Viability and Apoptosis Assay

To evaluate the possible cell viability effect of Se-BDEVs and cBDEVs, 293T cells or PANC-1 cells were seeded at a density of 1×10^4 cells in a 96-well-plate and incubated with Se-BELNs or cBELNs at different concentrations (0, 10, 20, and 40 ng/μL) for 12, 24, 48, and 72 h at 37°C. Then, cell viability was assessed using the Cell Counting Kit-8 (CCK-8, Vazyme, China).

For apoptosis assay, PANC-1 cells were firstly transfected with miR167a mimics, miR167a mimics combined with miR167a inhibitor (mimics + inhibitor), or miR167a negative control (NC), for 24 h, respectively. Then, cell apoptosis was assessed using the Annexin V/PI apoptosis detection kit (Yeasen, China) based on the manufacturer's instructions.

RNA Extraction and Real Time-PCR

RNA extraction and real-time PCR were carried out as previously reported.[32] The sense and antisense primers for *IRS1, ERBB3, FGF5, FGF23*, and *PIK3CB* were listed in Table 1. *β-Actin* was used for normalization. All primers for RT-PCR were obtained from Tsingke Biotechnology Co., Ltd. (China).

MiRNA-Seq Analysis

For miRNA sequencing (miRNA-Seq), three Se-BELNs samples and two cBDEVs samples were prepared. For each sample, approximately 1 μg of total RNA was used to construct a small RNA library according to the protocol of TruSeq

Table 1 Sequences of Primers Used for Polymerase Chain Reaction

Gene	Primer Sequence (5'-3')
IRS1_F	CCCAGGACCCGCATTCAAA
IRS1_R	GGCGGTAGATACCAATCAGGT
ERBB3_F	CTTCCTGCAGTGGATTCGA
ERBB3_R	AGGTTGGGCAATGGTAGAG
FGF5_F	CACTGATAGGAACCCTAGAGGC
FGF5_R	CAGATGGAAACCGATGCCC
FGF23_F	CAGAGCCTATCCCAATGCCTC
FGF23_R	GGCACTGTAGATGGTCTGATGG
PIK3CB_F	TATTTGGACTTTGCGACAAGACT
PIK3CB_R	TCGAACGTACTGGTCTGGATAG
β-actin-F	CATGTACGTTGCTATCCAGGC
β-actin-R	CTCCTTAATGTCACGCACGAT

Small RNA Sample Prep Kits (Illumina, San Diego, USA). The miRNA-Seq data were subsequently processed using an in-house program, ACGT101-miR (LC Sciences, USA) following the vendor's recommended protocol.[33] Briefly, after removing 3' joint contamination data, low-quality data, sequences with a length less than 18 nt or larger than 25 nt, and non-coding RNAs (rRNA, tRNA, snRNA, and snoRNA), the remaining unannotated sequences were mapped to miRNA sequences in miRBase 21.0 database (https://www.mirbase.org/)[34] with the selected species as *Brassica oleracea*. All mapped miRNAs were identified as known miRNAs. Furthermore, the unmapped sequences were mapped to other known plant species (such as bol, aly, ath) and identified as candidate miRNAs. All miRNA profiling data have been deposited in NCBI-SRA (www.ncbi.nlm.nih.gov/sra, SRA accession: PRJNA825344) databases.

Firstly, the quality of each sequencing data was evaluated by principal component analysis (PCA). Then, the differential expression miRNAs (DEmiRNAs) between Se-BDEVs and cBDEVs based on normalized deep-sequencing counts were screened by using the Student's *t*-test with the threshold p-value < 0.05 and $|\log2FC| \geq 1$.

Bioinformatics Analysis

With miRNA-seq data, the human TGs prediction of annotated miRNAs was performed using TargetScan (v5.0) and miRanda (v3.3a). The thresholds for the algorithms were as follows: scores ≥ 90 for TargetScan; energy < -10 for miRanda; *Homo sapiens* as the species. In addition, KEGG pathway analysis and GO enrichment of miRNA TGs were performed using DAVID (https://david.ncifcrf.gov/) and visualized using OmicStudio tools at https://www.omicstudio.cn/tool/.

Protein-protein interaction (PPI) of the predicted TGs was constructed from the STRING database (http://string-db.org/) and visualized using Cytoscape (v3.7.1). Then, the Molecular Complex Detection (MCODE; v1.31) app in Cytoscape was used to analyze PPI network modules. Genes involved in the highest score cluster were considered hub genes.

Besides, the expression pattern of hub genes in pancreatic cancer tissues and normal tissues was predicted using the Gene Expression Profiling Interactive Analysis (GEPIA) database (http://gepia.cancer-pku.cn/).

Furthermore, The NCBI database and RNAhybrid (https://bibiserv.cebitec.uni-bielefeld.de/rnahybrid/) were used in combination to search for human mRNAs containing potential binding sites for plant miRNAs.

Statistical Analysis

All experiments were performed in triplicates and the data are presented as the mean ± SEM. Statistical differences in the results of RT-PCR and flow cytometry were evaluated by using the Student's *t*-test. Statistical differences for growth curves were evaluated by using two-way ANOVA. All p-values were calculated in GraphPad Prism software 8.1 (GraphPad Software Inc., USA). The $p < 0.05$ was considered statistically significant.

Results

Characterization and Uptake of Se-BDEVs and cBDEVs

Firstly, Se-BDEVs and cBDEVs were isolated from fresh broccoli using a differential centrifugation method (Figure 1). Then, we used NTA and TEM to identify the characterization of Se-BDEVs and cBDEVs. NTA consistently found abundant EVs with diameters from 50 to 150 nm in both Se-BDEVs and cBDEVs, and the primary peak of the particle size of Se-BDEVs is 127.1 nm, while that of cBDEVs is 117.4 nm (Figure 2A and Figure 2B). Similarly, TEM analysis of EVs pellets revealed a round-shaped membrane-bound structure about 100 nm in diameter (Figure 2C and Figure 2D). These observations indicated that EVs were successfully isolated from conventional broccoli and Se-enriched broccoli.

To further examine whether Se-BDEVs or cBDEVs could be taken up by mammalian cells, PKH26-labeled BDEVs were incubated with 293T cells at graded concentrations (10, 20, and 40 ng/μL). After 24 h incubation, fluorescent results showed that both Se-BDEVs and cBDEVs were taken up in a concentration-dependent manner by 293T cells (Figure S1).

MiRNA-Seq Analysis of Se-BDEVs and cBDEVs

MiRNAs are the dominant active ingredient in EVs, which have been frequently explored in previous studies in mammalian EVs. MiRNA-seq was used to replenish the role of miRNAs in Se-BDEVs and cBDEVs. To ensure accuracy and reliability, PCA was first used to evaluate the data distribution in each sample, and Se-BDEVs and cBDEVs had distinct component differences (Figure 3A). The heatmap then revealed that a total of 10 known miRNAs and 31 candidate miRNAs were annotated (Figure 3B and Supplementary Table 1).

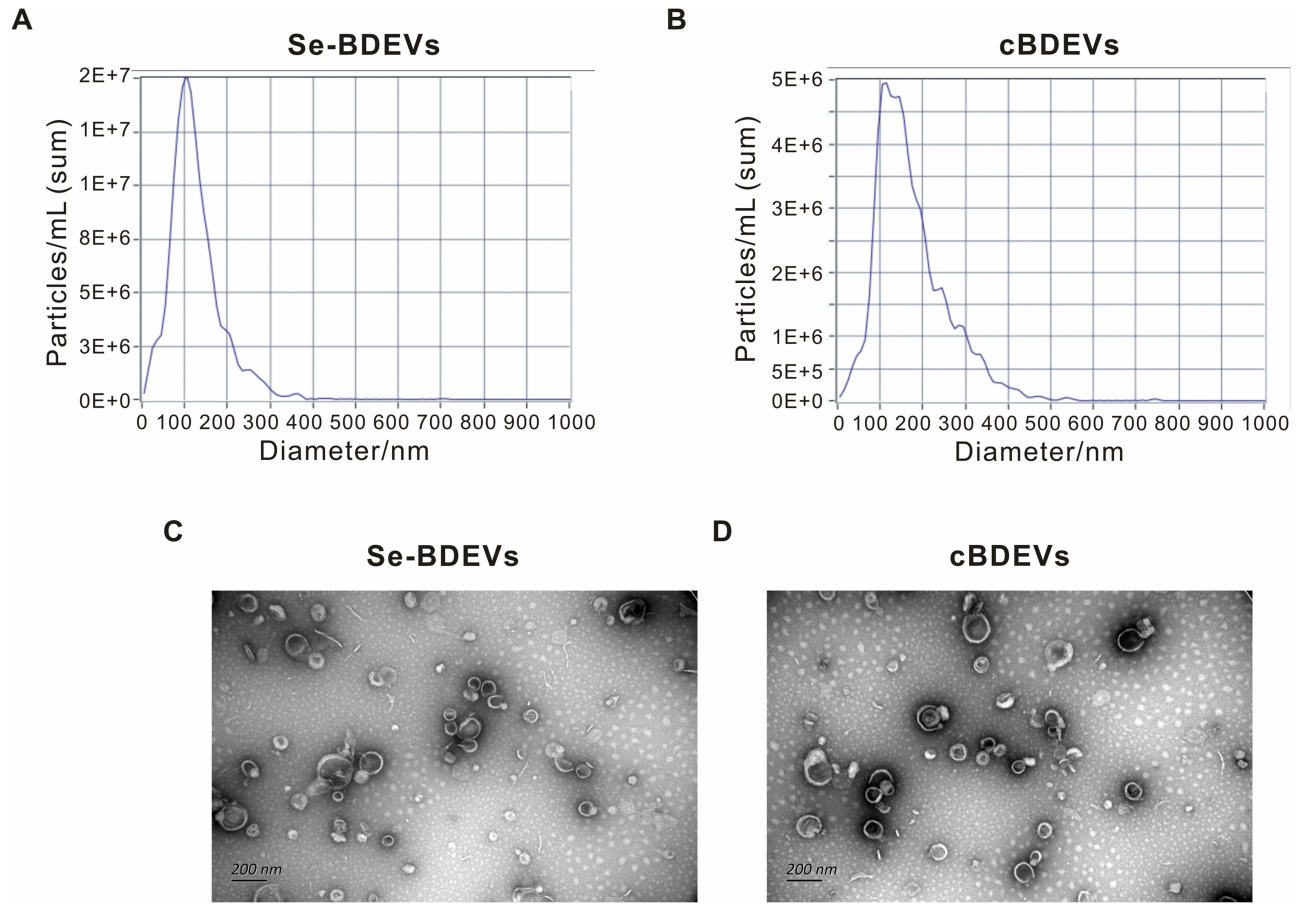

Figure 2 Characterization of extracellular vesicles derived from Se-riched broccoli (Se-BDEVs) and conventional broccoli (cBDEVs). (**A** and **B**) Extracellular vesicle size distribution and concentrations of Se-BDEVs and cBDEVs quantified by NTA. (**C** and **D**) Representative TEM images of Se-BDEVs and cBDEVs. Scale bar = 200 nm.

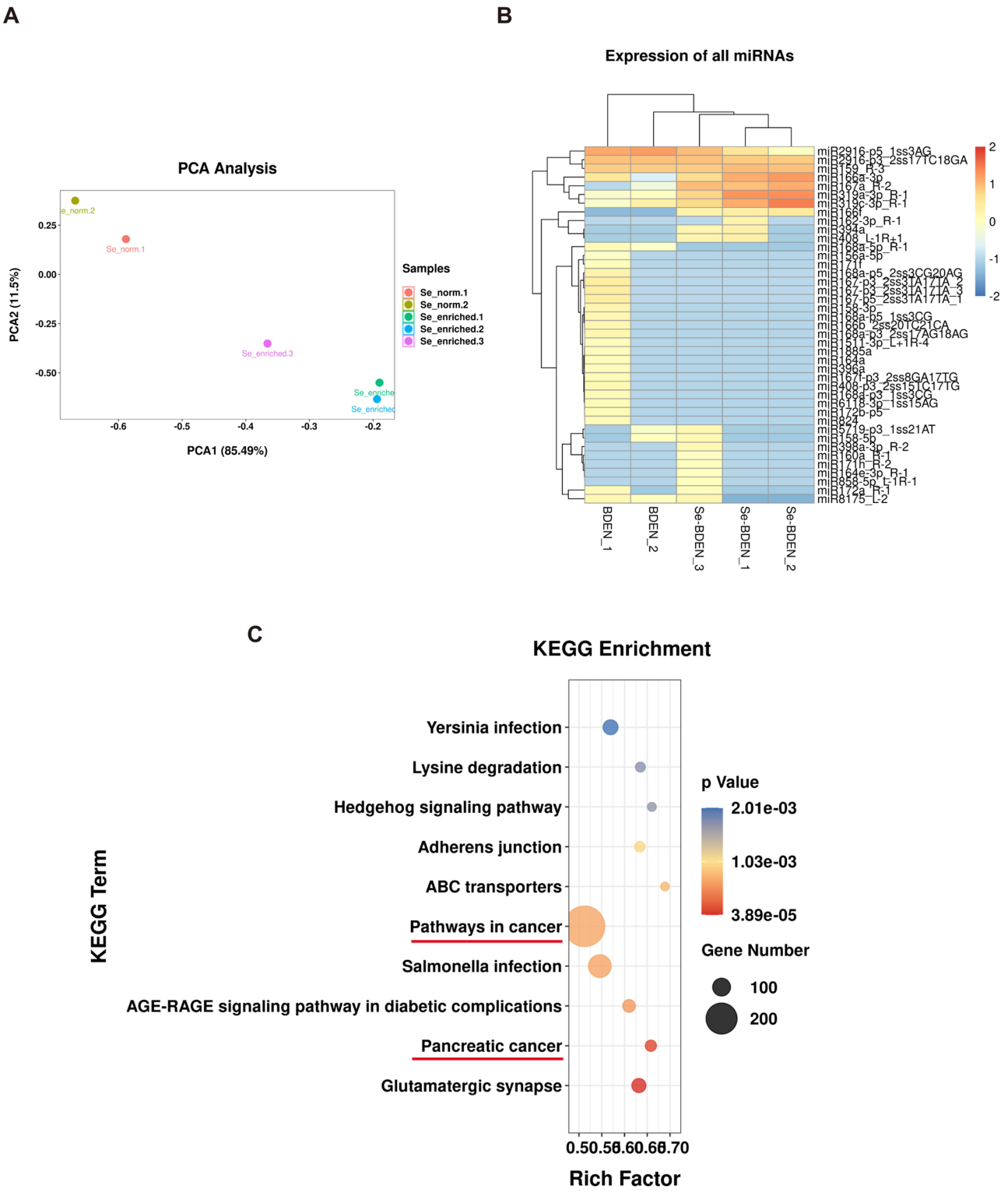

Figure 3 Analysis of miRNA-seq results. (**A**) Principal component analysis (PCA) analysis of Se-BDEVs (Se_enriched) and cBDEVs (Se-normal). (**B**) Heatmap of annotated miRNA expression in Se-BDEVs and cBDEVs. (**C**) KEGG enrichment analysis of miRNA target genes, with the top 10 most significantly enriched terms. Cancer-related pathways are marked with red lines.

Target Gene Prediction and Functional Analysis of Annotated miRNAs

Several recent studies have highlighted the cross-kingdom communication of plant-derived miRNAs and mammalian genes. However, the function of miRNAs derived from Se-BDEVs and cBDEVs, particularly their impact on human

genes, is still unknown. Thus, we predicted the TGs of the 41 annotated miRNAs (10 known miRNAs and 31 candidate miRNAs) targeting the human database and then examined their function to determine the competence of Se-BDEVs and cBDEVs. As a result, a total of 2556 TGs were discovered (Supplementary Table 2). Then, KEGG enrichment analysis was performed on these TGs, and the 10 most significantly enriched terms were shown in Figure 3C and Supplementary Table 3, with a threshold of $p < 0.001$. Notably, "Pancreatic cancer" is the second most significant KEGG pathway (based on the p value). What's more intriguing is that the pathway with the most genes is "pathway in cancer". Combining these results with previous studies on broccoli fighting cancer, we were inspired to further investigate the anti-pancreatic cancer effect of Se-BDEVs and cBDEVs.

Se-BDEVs Show A Stronger Anti-PAAD Potency Than cBDEVs

Next, we conducted experiments to verify the above bioinformatic analysis results. Indeed, the CCK-8 assay demonstrated that both Se-BDEVs and cBDEVs reduced the cell viability of PANC-1 in a concentration-dependent manner (Figure 4A and Figure 4B). Furthermore, Se-BDEVs suppressed cell viability more effectively than cBDEVs (Figure 4C). These findings demonstrated that both Se-BDEVs and cBDEVs have anti-PAAD effects, with Se-BDEVs being more potent.

In addition, PANC-1 cells were incubated with PKH67-labeled EVs for 30 min, 1 h, 2 h, 4 h, and 6 h to assay the uptake efficiency. As a result, we found that the number of PKH67 positive cells continued to increase with time regardless of whether the cells incubated with cBDEVs or Se-BDEVs. After 4 h of incubation, cellular uptake in both two groups reached saturation (Figure 4D and Figure 4E).

Differential Expression miRNAs Between Se-BDEVs and cBDEVs

To further explore which miRNAs mediate Se to enhance the anti-pancreatic cancer effect of broccoli-EVs, we conducted differential expression miRNA analysis between Se-BDEVs and cBDEVs. Compare to cBDEVs, one significantly down-regulated miRNA (peu-miR2916-p5_1ss3AG, fold change = 8.74, cBDEVs vs Se-BDEVs) and one significantly up-regulated miRNA (bna-miR167a_R-2, fold change = 41.03, Se-BDEVs vs cBDEVs) were obtained in Se-BDEVs (Figure 5A). Then, the TGs of peu-miR2916-p5_1ss3AG (miR2916-p5) and bna-miR167a_R-2 (miR167a) was predicted, resulting in 95 TGs of miR2916-p5 (Supplementary Table 4) and 678 TGs of miR167a (Supplementary Table 5).

Similar to the previous experiment, herein, we analyzed the functional enrichment associated with TGs of miR2916-p5 and miR167a to further clarify the functional miRNA. Go and KEGG analysis results showed that the functions of miR167a TGs, but not miR2916-p5 TGs (Figure S2), are closely related to cancer. Specifically, for the miR167a TGs, the most significant GO terms in BPs were "cell cycle" (Figure 5B and Supplementary Table 6), while the most significant KEGG enrichment pathway was "apoptosis" (Figure 5C and Supplementary Table 7). As we know, the important goal of anti-cancer therapy is to trigger apoptosis in oncocytes. Accordingly, we hypothesized that miR167a could limit pancreatic cancer cell survival by inducing apoptosis.

Effect of miR167a on Human Pancreatic Cancer Cell

To confirm the above hypothesis, we first confirm the enrichment of miR167a in Se-BDEVs and cBDEVs. As shown in Figure 6A, RT-PCR revealed that miR167a presented significantly lower Ct values in Se-BDEV compared to cBDEVs suggesting its higher expression in Se-BDEVs, corroborating with their relative expression in the miRNA-seq.

Then, we transfected PANC-1 cells with Se-BDEVs, cBDEVs, miR167a mimics, miRNA mimics + inhibitor, and miR167a NC, respectively. CCK-8 assay was used to detect the cell viability and the results showed that, after 24 and 48 h of transfection, miR167a mimics could dramatically reduce PANC-1 cell viability (Figure 6B and Figure 6C). Meanwhile, miR167a mimics also dramatically aggravate apoptosis after cells are transfected for 24 h when compared to miRNA mimics + inhibitor, NC, and control (Figure 6D–F). Together, these findings support the notion that substantially abundant miR167a in Se-BDEVs exerts an anti-pancreatic cancer cell effect via promoting apoptosis.

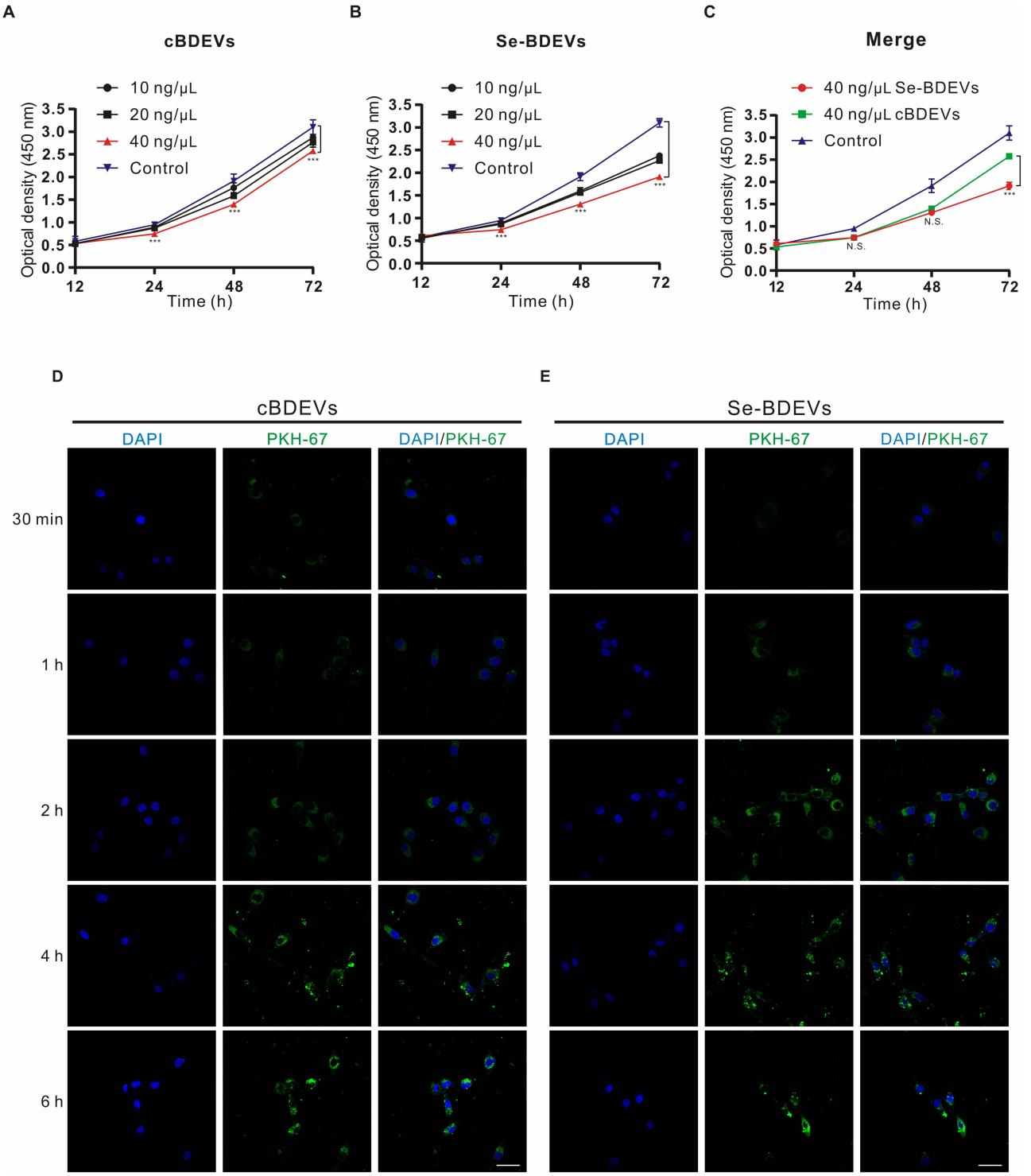

Figure 4 Effect of BDEVs and Se-BDEVs on the PANC-1. The cell viability was detected by CCK-8 and expressed as optical density (OD). (**A** and **B**) OD values were measured after subjecting PANC-1 cells with graded concentrations (0, 10, 20, and 40 ng/μL) of cBDEVs or Se-BDEVs, ***$p < 0.001$, 40 ng/μL vs 0 ng/μL (Control). (**C**) Merge of growth curves of PANC-1 cells treated with 40 ng/μL cBDEVs, 40 ng/μL Se-BDEVs and Control, ***$p < 0.001$, 40 ng/μL Se-BDEVs vs 40 ng/μL BDEVs. (**D** and **E**) PANC-1 cells were incubated with PKH67-labeled 40 ng/μL cBDEVs or Se-BDEVs for 30 min, 1 h, 2h, 4 h, and 6 h. Scale bar: 50 μm.

Hub Genes Identification and Function Enrichment Analysis

To dissect the mechanisms by which miR167a modulates cell apoptosis, we first built a PPI network of the miR167a TGs. The PPI network displayed 1458 nodes and 661 edges (Figure 7A). Subsequently, we used the MCODE plugin of Cytoscape to parse the PPI network, and the key module with the highest score (Score: 5) was selected, and genes

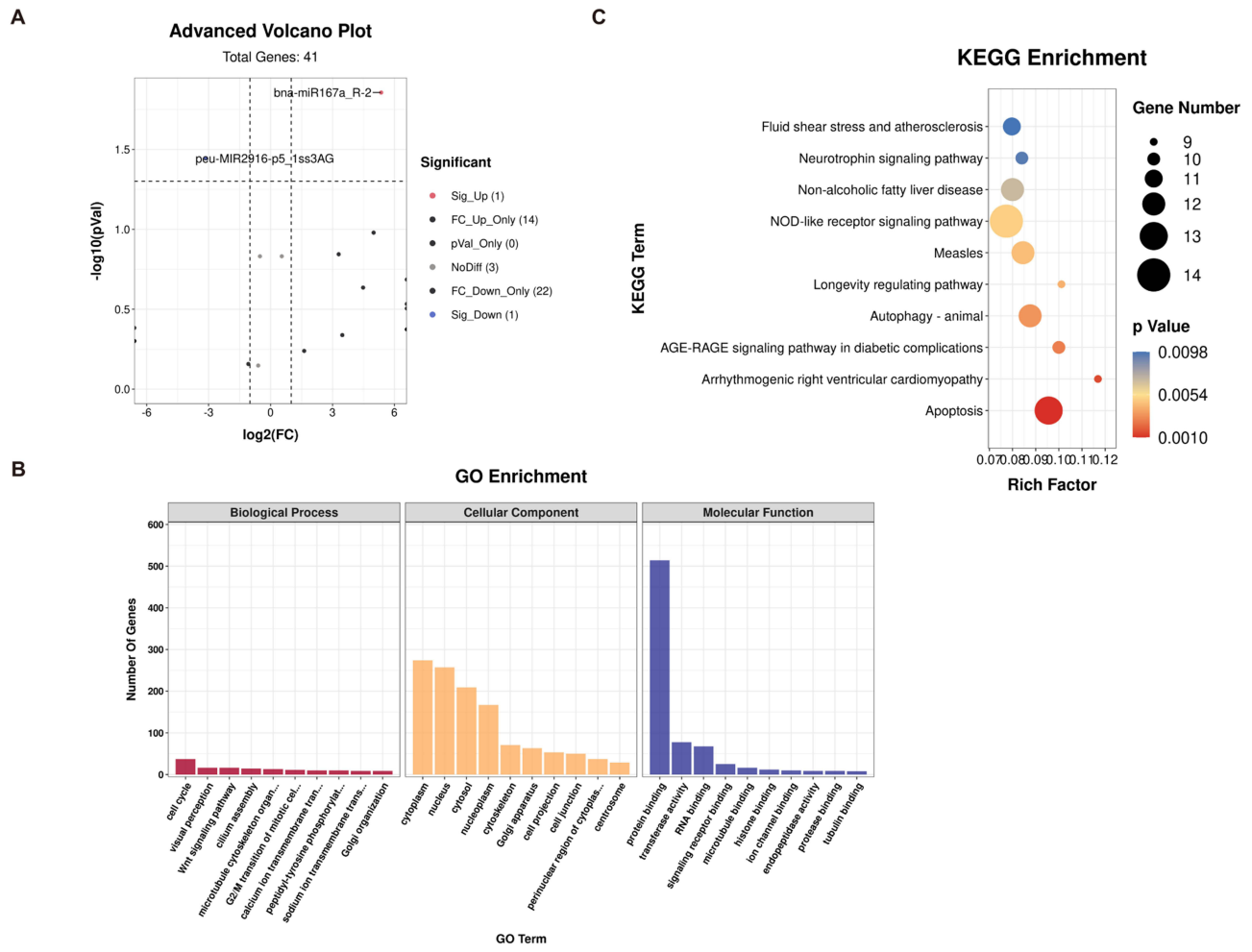

Figure 5 Target gene prediction of bna-miR167a_R-2 (miR167a) and functional enrichment analysis. (**A**) Volcano plots present the differential expression miRNAs between Se-BDEVs and cBDEVs. (**B**) GO analysis of miR167a target genes. (**C**) KEGG enrichment analysis of miR167a target genes.

involved in this module were dubbed hub genes, including Insulin Receptor Substrate 1 (*IRS1*), Erb-B2 Receptor Tyrosine Kinase 3 (*ERBB3*), Fibroblast Growth Factor 5 (*FGF5*), Fibroblast Growth Factor 23 (*FGF23*), and Phosphatidylinositol-4,5-Bisphosphate 3-Kinase Catalytic Subunit Beta (*PIK3CB*) (Figure 7B). Likewise, the functional annotation of the hub genes were analyzed using GO and KEGG enrichment, which revealed that those genes were enriched and played an essential part in "PI3K-AKT pathway" (Figure 7C and Figure 7D).

IRS1 is the Target of miR167a

Based on the above bioinformatics findings, we checked the expression levels of hub genes in the GEPIA database and found that expression of *ERBB3* and *IRS1* were significantly higher in PAAD tissue than in normal pancreatic tissue, whereas the other 3 hub genes (*FGF5, FGF23*, and *PIK3CB*) showed no significant difference (Figure 8A and Figure S3). Then, after transfecting PANC-1 with miR167a mimics, mimics + inhibitor, or NC, we used RT-PCR to confirm the expression level of those hub genes. When cells were transfected with miR167a mimics, *IRS1* expression was considerably lower than in the other groups (Figure 8B), however, the expression of the other four hub genes, ERBB3, FGF5, FGF23, and PIK3CB, did not alter significantly (Figure S4). These results indicate that only *IRS1* could be a possible target of miR167a.

Finally, we utilized the RNAhybrid bioinformatics program to see if miR167a could bind to *IRS1* and discovered that the seed sequence of miR167a was complementary to that of *IRS1* at two positions (Figure 8C and Figure 8D).

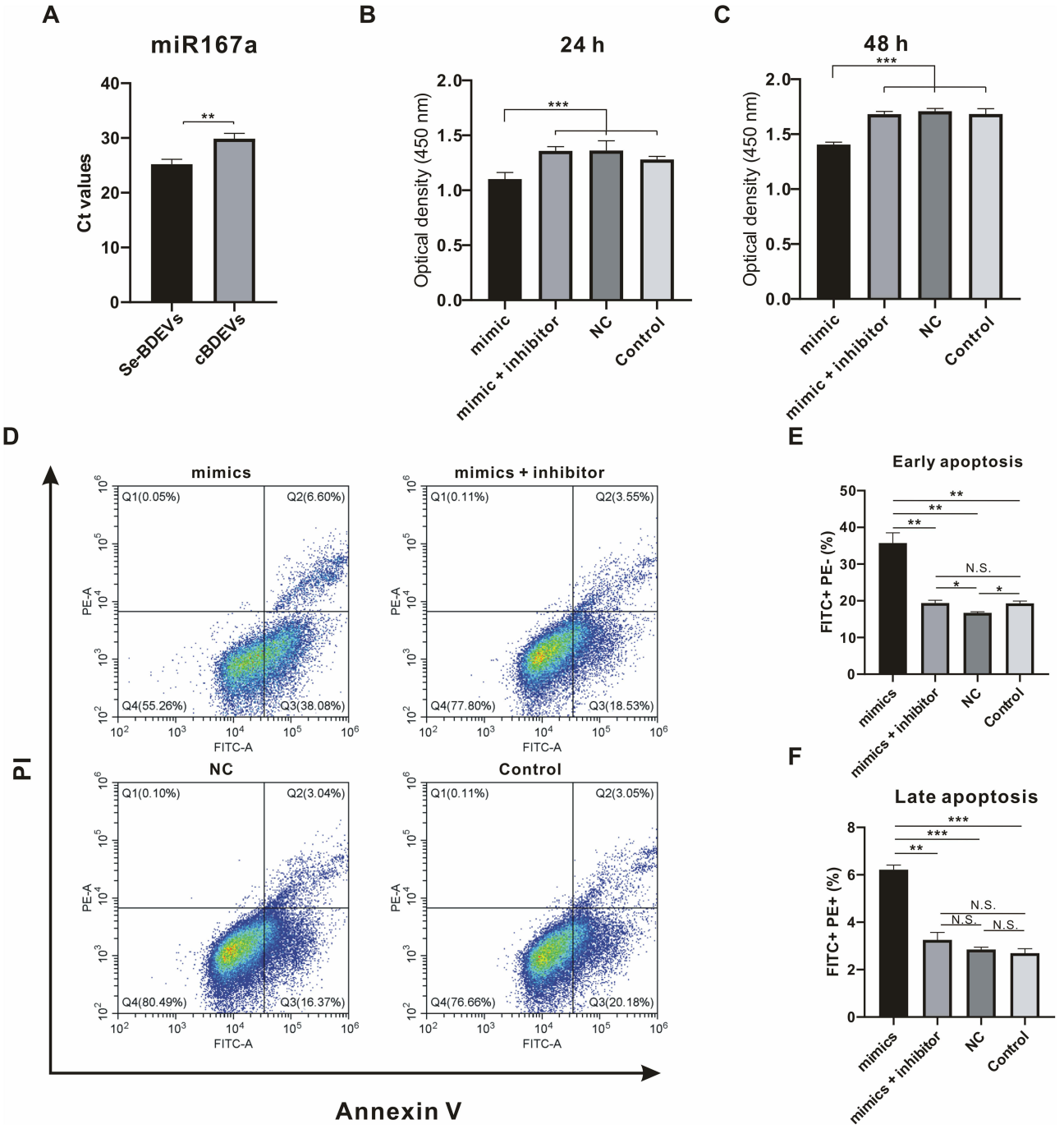

Figure 6 Effect of miR167a on PANC-1. (**A**) RT-PCR was utilized to detect the cycle threshold values (Ct) of miR167a in Se-BDEVs and cBDEVs. (**B** and **C**) Optical density presented the cell viability of PANC-1 cells transfected with miR167a mimics, miR167a mimics + inhibitor, miR167a NC, and control for 24 and 48 h. (**D**) Flow cytometry detected apoptosis rate after PANC-1 cells transfected with miR167a mimics, miR167a mimics + inhibitor, miR167a NC, and control for 24 h. (**E** and **F**) Statistical histogram of the apoptosis assay, $FITC^+PE^-$ was the percentage of early apoptotic cells, and $FITC^+PE^+$ was the percentage of late apoptotic cells. ***$p < 0.001$; **$p < 0.01$.
Abbreviations: N.S., not significant.

Discussion

In general, pancreatic cancer presents an exceptionally high morbidity and mortality rate, which poses a major health burden. Due to this, there has always been a focus on the utilization of diverse agents, such as fruits and vegetables and their derivatives, to prevent, inhibit, or reverse cancer development.[17,32,35] PDEVs are an emerging platform that has been recently discovered in a range of fruits and vegetables, including asparagus,[17] moringa oleifera,[36] and tea.[37] They

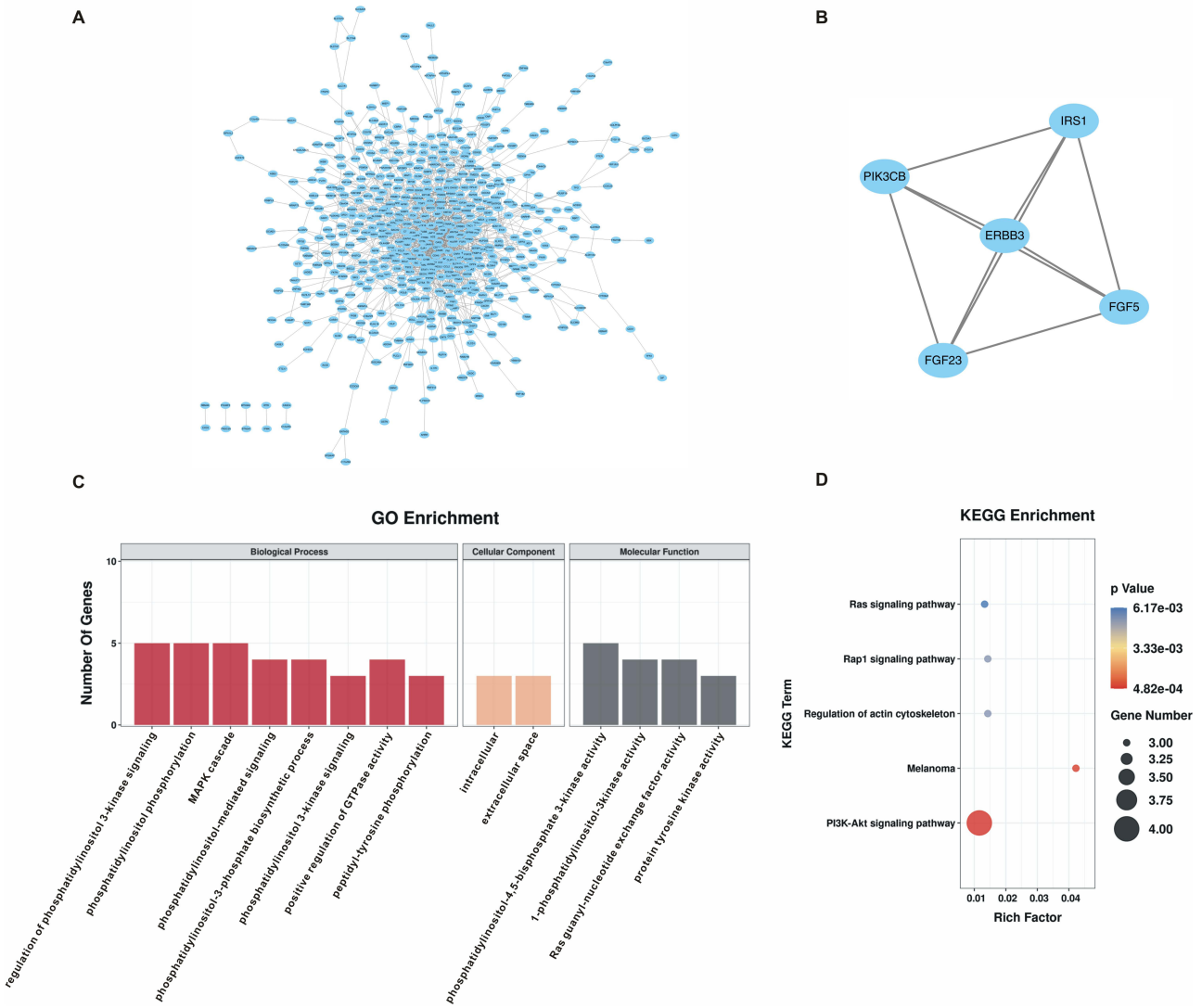

Figure 7 Hub genes identification and function enrichment analysis. (**A**) Protein-protein interaction (PPI) network of miR167a target genes. (**B**) The key module with the highest score (Score: 5) was analyzed by the Molecular Complex Detection (MCODE) in Cytoscape. Genes involved in this module were dubbed hub genes, including Insulin Receptor Substrate 1 (*IRS1*), Erb-B2 Receptor Tyrosine Kinase 3 (*ERBB3*), Fibroblast Growth Factor (*FGF*) 5, *FGF23*, and Phosphatidylinositol-4,5-Bisphosphate 3-Kinase Catalytic Subunit Beta (*PIK3CB*). (**C**) GO analysis of hub genes. (**D**) KEGG enrichment analysis of hub genes.

work cross-species in human cells and provide new cancer therapeutic possibilities.[17,36,38] In this study, we described the characterization of Se-BDEVs and cBDEVs, and found they may play a crucial role in treating pancreatic cancer. Moreover, we found that Se-BDEVs had a stronger anti-PAAD potency than cBDEVs because of the increased miR167a expression. Finally, our in vitro study demonstrated that miR167a induced PAAD apoptosis by targeting IRS1.

For the PDEVs isolation, previous research has shown the isolation methods and physicochemical properties of PDEVs are comparable to the mammalian EVs.[19] However, the presence of the cell wall may prevent the passage of EVs. So, in the first step of the isolation process, a blender is necessary to gently break the barrier of the cell wall, which is not required for mammalian EVs. Because of this distinction, we initially characterized our isolated Se-BDEVs and cBDEVs, and the results revealed that they have exosome-like properties, as previously reported.[39]

Plant miRNAs may play a physiologic role in mammalian cells.[38,40] For instance, plant miR159 was found to be capable of suppressing breast cancer proliferation by targeting TCF7.[40] Although the functionality of compounds in BDEVs has been explored in recent studies,[18,28] the role of miRNAs has not yet been considered. Herein, we investigated the functional characteristics of obtained Se-BDEVs and cBDEVs using miRNA-seq and miRNA TGs prediction as

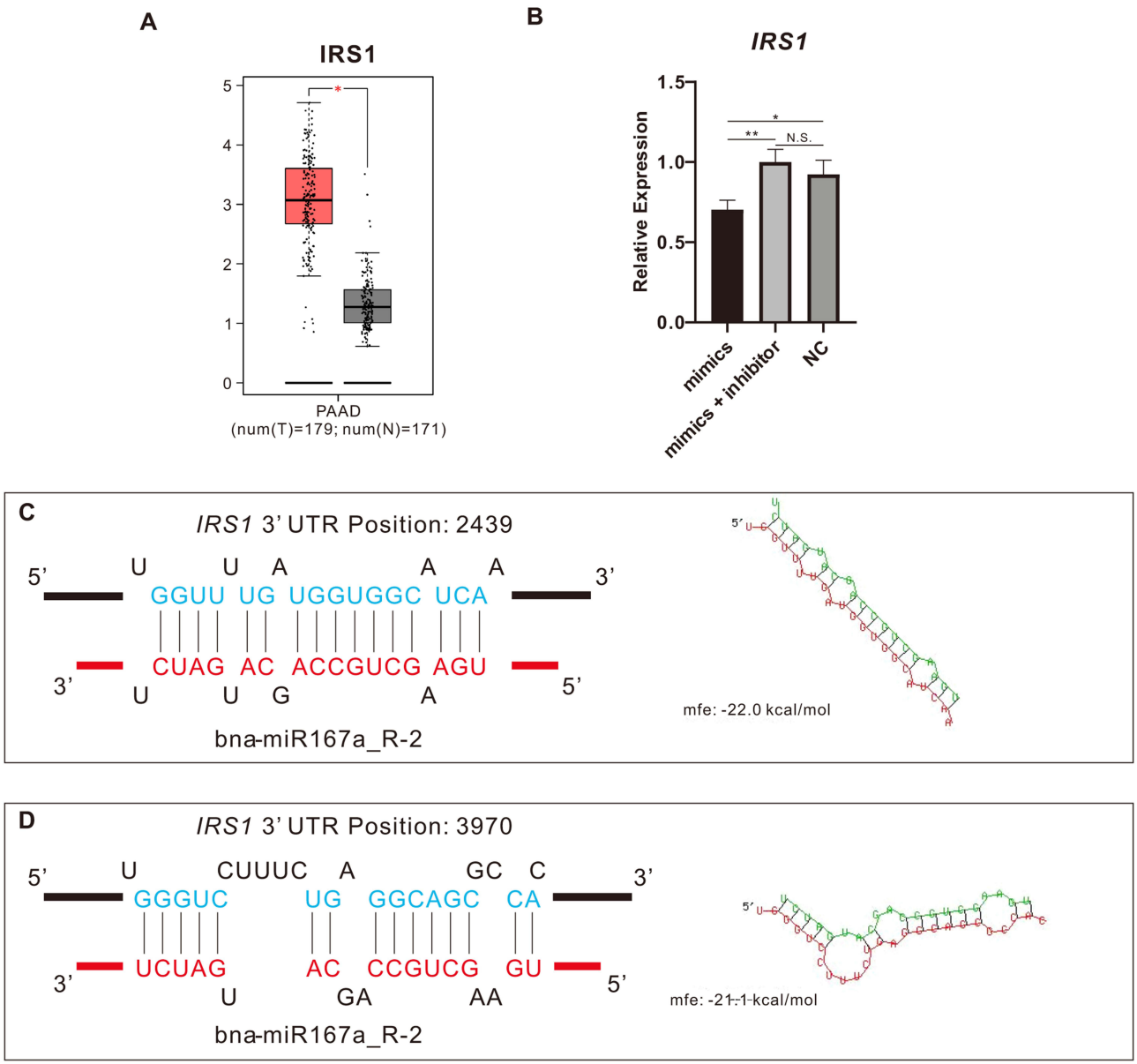

Figure 8 Mir167a binds *IRS1*. (**A**) Gene Expression Profiling Interactive Analysis (GEPIA) was utilized for analyzing *IRS1* expression in pancreatic adenocarcinoma (PAAD) and normal tissues. (**B**) RT-PCR was utilized for detecting *IRS1* expression in PANC-1 cells transfected with miR167a mimics, miR167a mimics + inhibitor, and miR167a NC, respectively. (**C** and **D**) MiR167a binding with *IRS1* predicted by RNAhybrid. *IRS1* contains two sites complementary to the seed sequence of miR167a. *$p < 0.05$, **$p<0.01$. **Abbreviations**: N.S., not significant.

many previous studies did.[41] Interestingly, our functional enrichment study showed that miRNAs in BDEVs were predominantly enriched in anti-cancer biological pathways, with a particular emphasis on pancreatic cancer (Figure 3C). Based on this discovery, we validated the bioinformatic data using a pancreatic cancer cell line (PANC-1). Both Se-BDEVs and cBDEVs significantly reduced the viability of PANC-1 cells (Figure 4A and Figure 4B). The use of broccoli sprouts to treat pancreatic cancer has yielded positive effects, albeit there are some side effects and drawbacks at large doses.[24] Nevertheless, PDEVs, a highly concentrated plant by-product, possess far higher bioactivity than what can be achieved through dietary intake.[13] Thus, small dosages of PDEVs may have strong anti-cancer effects. In addition, Se biofortification has also been frequently reported to improve the effectiveness of broccoli. The strong alliance between BDEVs and Se biofortification may exert more unexpected effects. As we expected, Se-BDEVs had a stronger anti-PAAD effect than cBDEVs (Figure 4C).

Given the above finding, the differential expression of miRNAs between Se-BDEVs and cBDEVs was investigated. As a result, one miRNA was found to be significantly down-regulated (peu-miR2916-p5 1ss3AG) while one miRNA was found to be significantly up-regulated (bna-miR167a R-2) (Figure 5A). Similarly, for these two miRNAs, we did TGs prediction and functional enrichment analysis, respectively. The results showed that the function of miR2916-p5 TGs is unrelated to cancer (Figure S2), but miR167a TGs are involved in the apoptotic pathway (Figure 5C). Apoptosis induction is a well-known anticancer strategy.[42] Meanwhile, since Se-BDEVs had a stronger effect than cBDEVs, we hypothesized that it was due to increased substances overexpression of miR167a in PANC-1 causing cell apoptosis (Figure 6D–F). Collectively, these data support that BDEVs are implicated in cancer viability, and that Se enrichment enhances this effect.

Subsequently, we investigated the hub genes of miR167a TGs as previous studies reported. Since miRNAs play a role in limiting mRNA expression, we discovered that *IRS1* and *ERBB3* were significantly overexpressed in PAAD tissue relative to normal tissue in the TCGA database (Figure 8A and Figure S3). Moreover, our RT-PCR results confirmed that miR167a selectively inhibits IRS1 expression in PANC-1 cells (Figure 8B and Figure S4). IRS1, the first identified member of the IRS family, was initially thought to be a typical cytolytic adaptor protein.[43] Many studies also demonstrated that up-regulated IRS1 plays a key role in transmitting signals from oncogenic insulin-like growth factor (IGF) receptors to the intracellular PI3K/Akt pathway in numerous cancers, including pancreatic cancer.[44,45] Then, the analysis of miRNA binding site also demonstrated that there are two miR167a binding sites at the 3′UTR of *IRS1* (Figure 8C and Figure 8D).

However, this study has several limitations. First, future research should explore whether BDEVs influence the function of other pancreatic cancer cells. Second, the mechanisms underlying our study were not thoroughly investigated, particularly in terms of validating the function and mechanism of miR167a in animal models or even humanized models.

Conclusions

We have defined the biological properties of Se-BDEVs and cBDEVs, and found that miR167a targeting IRS1 is the key mechanism that exerts an anti-PAAD effect. These findings may pave the way for the regulation of Se-BDEVs, cBDEVs, and plant-derived miRNAs in human cancer.

Acknowledgments

This study was supported by the National Key R&D Program of China (grant number: 2022YFA0806100), the Natural Science Foundation of Enshi Government (grant number: E20190002), the National Natural Science Foundation of China (grant number: 82070808, 82100931, and 82104302), and the Fundamental Research Funds of the Central Universities (HUST: 2022JYCXJJ050). The authors also thank the Figdraw (www.figdraw.com) for providing the elements in the figures.

Disclosure

The authors declare no competing financial interest.

References

1. Falasca M, Kim M, Casari I. Pancreatic cancer: current research and future directions. *Biochim Biophys Acta*. 2016;1865(2):123–132. doi:10.1016/j.bbcan.2016.01.001
2. Hosein AN, Brekken RA, Maitra A. Pancreatic cancer stroma: an update on therapeutic targeting strategies. *Nat Rev Gastroenterol Hepatol*. 2020;17(8):487–505. doi:10.1038/s41575-020-0300-1
3. Matera R, Saif MW. New therapeutic directions for advanced pancreatic cancer: cell cycle inhibitors, stromal modifiers and conjugated therapies. *Expert Opin Emerg Drugs*. 2017;22(3):223–233. doi:10.1080/14728214.2017.1362388
4. Rezaie J, Ahmadi M, Ravanbakhsh R, et al. Tumor-derived extracellular vesicles: the metastatic organotropism drivers. *Life Sci*. 2022;289:120216. doi:10.1016/j.lfs.2021.120216
5. Hassanpour M, Rezaie J, Darabi M, Hiradfar A, Rahbarghazi R, Nouri M. Autophagy modulation altered differentiation capacity of CD146(+) cells toward endothelial cells, pericytes, and cardiomyocytes. *Stem Cell Res Ther*. 2020;11(1). doi:10.1186/s13287-020-01656-0
6. Rahbarghazi R, Jabbari N, Sani NA, et al. Tumor-derived extracellular vesicles: reliable tools for Cancer diagnosis and clinical applications. *Cell Commun Signal*. 2019;17(1):73. doi:10.1186/s12964-019-0390-y
7. Nikfarjam S, Rezaie J, Zolbanin NM, Jafari R. Mesenchymal stem cell derived-exosomes: a modern approach in translational medicine. *J Transl Med*. 2020;18(1):449. doi:10.1186/s12967-020-02622-3

8. Vahabi A, Rezaie J, Hassanpour M, et al. Tumor cells-derived exosomal CircRNAs: novel cancer drivers, molecular mechanisms, and clinical opportunities. *Biochem Pharmacol*. 2022;200:115038. doi:10.1016/j.bcp.2022.115038
9. Joo HS, Suh JH, Lee JM, Bang ES, Lee JM. Current knowledge and future perspectives on mesenchymal stem cell-derived exosomes as a new therapeutic agent. *Int J Mol Sci*. 2020;21(3):727. doi:10.3390/ijms21030727
10. EL Andaloussi S, Mäger I, Breakefield XO, Wood MJA. Extracellular vesicles: biology and emerging therapeutic opportunities. *Nat Rev Drug Discov*. 2013;12(5):347–357. doi:10.1038/nrd3978
11. Xiao J, Feng S, Wang X, et al. Identification of exosome-like nanoparticle-derived microRNAs from 11 edible fruits and vegetables. *PeerJ*. 2018;6:e5186. doi:10.7717/peerj.5186
12. Feghhi M, Rezaie J, Akbari A, et al. Effect of multi-functional polyhydroxylated polyhedral oligomeric silsesquioxane (POSS) nanoparticles on the angiogenesis and exosome biogenesis in human umbilical vein endothelial cells (HUVECs). *Mater Design*. 2021;20:197.
13. Nemati M, Singh B, Mir RA, et al. Plant-derived extracellular vesicles: a novel nanomedicine approach with advantages and challenges. *Cell Commun Signal*. 2022;20(1):69. doi:10.1186/s12964-022-00889-1
14. Baldini N, Torreggiani E, Roncuzzi L, Perut F, Zini N, Avnet S. Exosome-like nanovesicles isolated from citrus limon L. exert antioxidative effect. *Curr Pharm Biotechnol*. 2018;19(11):877–885. doi:10.2174/1389201019666181017115755
15. Zhang M, Viennois E, Xu C, Merlin D. Plant derived edible nanoparticles as a new therapeutic approach against diseases. *Tissue Barriers*. 2016;4(2):e1134415. doi:10.1080/21688370.2015.1134415
16. Mu J, Zhuang X, Wang Q, et al. Interspecies communication between plant and mouse gut host cells through edible plant derived exosome-like nanoparticles. *Mol Nutr Food Res*. 2014;58(7):1561–1573. doi:10.1002/mnfr.201300729
17. Zhang L, He F, Gao L, et al. Engineering exosome-like nanovesicles derived from Asparagus cochinchinensis can inhibit the proliferation of hepatocellular carcinoma cells with better safety profile. *Int J Nanomedicine*. 2021;16:1575–1586. doi:10.2147/IJN.S293067
18. Yepes-Molina L, Carvajal M. Nanoencapsulation of sulforaphane in broccoli membrane vesicles and their in vitro antiproliferative activity. *Pharm Biol*. 2021;59(1):1490–1504. doi:10.1080/13880209.2021.1992450
19. Kim J, Li S, Zhang S, Wang J. Plant-derived exosome-like nanoparticles and their therapeutic activities. *Asian J Pharm Sci*. 2022;17(1):53–69. doi:10.1016/j.ajps.2021.05.006
20. Chen N, Sun J, Zhu Z, Cribbs AP, Xiao B. Edible plant-derived nanotherapeutics and nanocarriers: recent progress and future directions. *Expert Opin Drug Deliv*. 2022;19:409–419. doi:10.1080/17425247.2022.2053673
21. Suharta S, Barlian A, Hidajah AC, et al. Plant-derived exosome-like nanoparticles: a concise review on its extraction methods, content, bioactivities, and potential as functional food ingredient. *J Food Sci*. 2021;86(7):2838–2850. doi:10.1111/1750-3841.15787
22. Kapusta-Duch J, Kopec A, Piatkowska E, Borczak B, Leszczynska T. The beneficial effects of Brassica vegetables on human health. *Rocz Panstw Zakl Hig*. 2012;63(4):389–395.
23. Charron CS, Vinyard BT, Ross SA, Seifried HE, Jeffery EH, Novotny JA. Absorption and metabolism of isothiocyanates formed from broccoli glucosinolates: effects of BMI and daily consumption in a randomised clinical trial. *Br J Nutr*. 2018;120(12):1370–1379. doi:10.1017/S0007114518002921
24. Lozanovski VJ, Polychronidis G, Gross W, et al. Broccoli sprout supplementation in patients with advanced pancreatic cancer is difficult despite positive effects-results from the POUDER pilot study. *Invest New Drugs*. 2020;38(3):776–784. doi:10.1007/s10637-019-00826-z
25. Saeedi M, Soltani F, Babalar M, Izadpanah F, Wiesner-Reinhold M, Baldermann S. Selenium fortification alters the growth, antioxidant characteristics and secondary metabolite profiles of cauliflower (Brassica oleracea var. botrytis) cultivars in hydroponic culture. *Plants*. 2021;10(8):1537. doi:10.3390/plants10081537
26. Gui JY, Rao S, Gou Y, Xu F, Cheng S. Comparative study of the effects of selenium yeast and sodium selenite on selenium content and nutrient quality in broccoli florets (Brassica oleracea L. var. italica). *J Sci Food Agric*. 2022;102(4):1707–1718. doi:10.1002/jsfa.11511
27. Abdulah R, Faried A, Kobayashi K, et al. Selenium enrichment of broccoli sprout extract increases chemosensitivity and apoptosis of LNCaP prostate cancer cells. *BMC Cancer*. 2009;9:414. doi:10.1186/1471-2407-9-414
28. Deng Z, Rong Y, Teng Y, et al. Broccoli-derived nanoparticle inhibits mouse colitis by activating dendritic cell AMP-activated protein kinase. *Mol Ther*. 2017;25(7):1641–1654. doi:10.1016/j.ymthe.2017.01.025
29. Jin J, Qian F, Zheng D, He W, Gong J, He Q. Mesenchymal stem cells attenuate renal fibrosis via exosomes-mediated delivery of microRNA Let-7i-5p antagomir. *Int J Nanomedicine*. 2021;16:3565–3578. doi:10.2147/IJN.S299969
30. Yin L, Yan L, Yu Q, et al. Characterization of the MicroRNA profile of ginger exosome-like nanoparticles and their anti-inflammatory effects in intestinal Caco-2 cells. *J Agric Food Chem*. 2022. 2022:145
31. Yue T, Sun F, Wang F, et al. MBD2 acts as a repressor to maintain the homeostasis of the Th1 program in type 1 diabetes by regulating the STAT1-IFN-gamma axis. *Cell Death Differ*. 2021;29:218–229. doi:10.1038/s41418-021-00852-6
32. Sun F, Wang FX, Zhu H, et al. SUMOylation of PDPK1 is required to maintain glycolysis-dependent CD4 T-cell homeostasis. *Cell Death Dis*. 2022;13(2):181. doi:10.1038/s41419-022-04622-1
33. Sun W, Xu XH, Wu X, et al. Genome-wide identification of microRNAs and their targets in wild type and phyB mutant provides a key link between microRNAs and the phyB-mediated light signaling pathway in rice. *Front Plant Sci*. 2015;6:372. doi:10.3389/fpls.2015.00372
34. Haunsberger SJ, Connolly NM, Prehn JH. miRNAmeConverter: an R/bioconductor package for translating mature miRNA names to different miRBase versions. *Bioinformatics*. 2017;33(4):592–593. doi:10.1093/bioinformatics/btw660
35. Tomita LY, Horta BL, da Silva LLS, Malta MB, Franco EL, Cardoso MA. Fruits and vegetables and cervical cancer: a systematic review and meta-analysis. *Nutr Cancer*. 2021;73(1):62–74. doi:10.1080/01635581.2020.1737151
36. Potesta M, Roglia V, Fanelli M, et al. Effect of microvesicles from Moringa oleifera containing miRNA on proliferation and apoptosis in tumor cell lines. *Cell Death Discov*. 2020;6:43. doi:10.1038/s41420-020-0271-6
37. Chen Q, Li Q, Liang Y, et al. Natural exosome-like nanovesicles from edible tea flowers suppress metastatic breast cancer via ROS generation and microbiota modulation. *Acta Pharmaceutica Sinica B*. 2022;12(2):907–923. doi:10.1016/j.apsb.2021.08.016
38. Zhou Q, Ma K, Hu H, Xing X, Huang X, Gao H. Extracellular vesicles: their functions in plant-pathogen interactions. *Mol Plant Pathol*. 2021;23:760–771. doi:10.1111/mpp.13170
39. Trentini M, Zanotti F, Tiengo E, et al. An apple a day keeps the doctor away: potential role of miRNA 146 on macrophages treated with exosomes derived from apples. *Biomedicines*. 2022;10(2):415. doi:10.3390/biomedicines10020415

40. Chin AR, Fong MY, Somlo G, et al. Cross-kingdom inhibition of breast cancer growth by plant miR159. *Cell Res*. 2016;26(2):217–228. doi:10.1038/cr.2016.13
41. Zhou J, Zhao H, Zhang L, et al. Integrated analysis of RNA-seq and microRNA-seq depicts miRNA-mRNA networks involved in stripe patterns of Botia superciliaris skin. *Funct Integr Genomics*. 2019;19(5):827–838. doi:10.1007/s10142-019-00683-2
42. Chen X, Zeh HJ, Kang R, Kroemer G, Tang D. Cell death in pancreatic cancer: from pathogenesis to therapy. *Nat Rev Gastroenterol Hepatol*. 2021;18(11):804–823. doi:10.1038/s41575-021-00486-6
43. Parathath SR, Mainwaring LA, Fernandez LA, Campbell DO, Kenney AM. Insulin receptor substrate 1 is an effector of sonic hedgehog mitogenic signaling in cerebellar neural precursors. *Development*. 2008;135(19):3291–3300. doi:10.1242/dev.022871
44. Li J, Su L, Gong YY, et al. Downregulation of miR-139-5p contributes to the antiapoptotic effect of liraglutide on the diabetic rat pancreas and INS-1 cells by targeting IRS1. *PLoS One*. 2017;12(3):e0173576. doi:10.1371/journal.pone.0173576
45. Xia W, Jie W. ZEB1-AS1/miR-133a-3p/LPAR3/EGFR axis promotes the progression of thyroid cancer by regulating PI3K/AKT/mTOR pathway. *Cancer Cell Int*. 2020;20(1). doi:10.1186/s12935-020-1098-1